


Cite this: *RSC Adv.*, 2024, 14, 17480

# A simple and efficient synthesis of 5-hydroxymethylfurfural from carbohydrates using acidic ionic liquid grafted on silica gel†

Vinh Thanh Chau Doan,<sup>abc</sup> Thong Minh Dao,<sup>ac</sup> Thu Anh Huynh,<sup>ac</sup> The Thai Nguyen<sup>ac</sup> and Phuong Hoang Tran<sup>id</sup> \*<sup>ac</sup>

The catalytic application of 3-(4-sulfobutyl)-1*H*-imidazole-3-ium chloride immobilized on activated silica gel (SiO<sub>2</sub>-Imi-SO<sub>3</sub>H) for the production of 5-hydroxymethylfurfural is described here for the first time. This material was synthesized using a three-step method involving the grafting of chloropropyl groups onto activated silica gel, the substitution of zwitterions, and the acidification of zwitterions to form silica-supported ionic liquid. The successful immobilization of the IL on silica gel was confirmed through energy-dispersive X-ray (EDX) spectroscopy, Fourier transform infrared spectroscopy (FT-IR), X-ray diffraction (XRD), scanning electron microscopy (SEM), and elemental mapping. SiO<sub>2</sub>-Imi-SO<sub>3</sub>H-2 demonstrated good catalytic activity and recycling ability in fructose dehydration to 5-HMF. Several conditions for reaction were investigated, and an excellent 5-HMF yield (94.1%) was obtained after 4 h at 160 °C in dimethyl sulfoxide (DMSO) from fructose. Furthermore, a mechanism was proposed, the catalyst's reusability was investigated, and the catalyst was applied for the conversion of glucose to 5-HMF with other metal salts.

Received 2nd April 2024

Accepted 21st May 2024

DOI: 10.1039/d4ra02487g

rsc.li/rsc-advances

## Introduction

Currently, the world's need for petroleum and chemical products is increasing, but fossil fuel reserves are progressively depleting. As a result, the search for renewable sources to replace fossil resources in manufacturing not only fuels but also chemicals has captured the interest of scientists and government officials.<sup>1</sup> In this sense, 5-hydroxymethylfurfural (5-HMF) has captured the curiosity of many as a substrate for the synthesis of different chemicals and liquid transportation fuels.<sup>2–5</sup> The most often reported method for producing 5-HMF is dehydration of carbohydrates catalyzed by acid.<sup>6–8</sup> Various acid catalysts such as mineral acids,<sup>9</sup> organic acids,<sup>10</sup> H-form zeolites,<sup>11</sup> transition metal ions,<sup>12</sup> solid metal phosphates,<sup>13–15</sup> and acidic cation exchange resins<sup>16–19</sup> have been employed in the production of 5-HMF using fructose as the catalysts. In the utilization of mineral acids, namely H<sub>2</sub>SO<sub>4</sub>, H<sub>3</sub>PO<sub>4</sub>, or HCl, as catalysts for the conversion of fructose to 5-HMF within a blend of organic solvent and DMSO at a pH level of 1.0 and a temperature of 413 K, an observed 5-HMF selectivity of 89% was achieved.<sup>9</sup> Subsequently, Sajid employed oxalic acid as a catalyst for the

dehydration of fructose. This process was conducted at 130 °C for a duration of 2 h within the medium of DMSO, resulting in an attained 5-HMF yield of 84.1%.<sup>10</sup> However, homogeneous acids have serious drawbacks in terms of the complex separation and recovery, pollution, and corrosion. Scientists have recently concentrated on using heterogeneous acidic catalysts for 5-HMF formation.<sup>20–22</sup> Heterogeneous catalysts modified with sulfonic acid are considered effective because of their high activity, high acid strength, ease of handling, and simple production technique. Heterogeneous catalysts are frequently recycled more readily,<sup>23</sup> and recovery strategies utilizing filtering or centrifugation to reduce the number of catalysts have been suggested utilizing this approach.<sup>24</sup> A carbonaceous catalyst containing the –SO<sub>3</sub>H group was utilized in the dehydration process of fructose within a DMSO medium under microwave irradiation. This method yielded a 79.9% 5-HMF output; however, the catalyst demonstrated poor reusability.<sup>25</sup> In another study, Zhao *et al.* developed a solid heteropolyacid catalyst, Cs<sub>2.5</sub>H<sub>0.5</sub>PW<sub>12</sub>O<sub>40</sub>, for fructose dehydration within a biphasic system. They achieved a 5-HMF yield of 74.0% under conditions of 388 K for 1 h. Notably, the composition of this catalyst was significantly more complex.<sup>26</sup> Because of their unique properties, such as large surface area, homogeneous distribution of pore sizes, cheap cost, and good thermal resistance, silica materials are good candidates for –SO<sub>3</sub>H group immobilization among several catalytic supports.

Ionic liquids (ILs) have received considerable interest over the past few decades as environmentally benign reaction media

<sup>a</sup>Department of Organic Chemistry, Faculty of Chemistry, University of Science, Ho Chi Minh City, Vietnam. E-mail: thphuong@hcmus.edu.vn

<sup>b</sup>Faculty of Interdisciplinary Science, University of Science, Ho Chi Minh City, Vietnam

<sup>c</sup>Vietnam National University, Ho Chi Minh City, Vietnam

† Electronic supplementary information (ESI) available. See DOI: <https://doi.org/10.1039/d4ra02487g>



due to their unique qualities of great thermal durability, minimal pressure of vapor, variable pH values, and selective solvability.<sup>27,28</sup> Huang *et al.* documented the synthesis of a functionalized diallylimidazolium ionic liquid and its subsequent use in the conversion process of fructose under microwave irradiation. This approach yielded a 73.7% 5-HMF with DMSO medium.<sup>29</sup> Eminov and coworkers utilized the ionic liquid  $[C_4C_1im][HSO_4]$  in conjunction with  $CrCl_3$  salt to convert fructose into 5-HMF. This reaction was conducted at 100 °C for 3 h, resulting in an impressive 96% yield of 5-HMF.<sup>30</sup> Despite such promising benefits, ILs' popular utilization was restricted by various limitations: (i) a high viscosity, resulting in only an IL amount participating in the catalysis process, (ii) homogeneous reaction, which made the separation of products and catalyst difficult, and (iii) subsequently expensive for the application of ILs in fairly significant quantities.<sup>31,32</sup> To address these issues, catalysts that combined the beneficial properties of ILs and solid acids were suggested.<sup>33</sup>

With all of these in mind, and as part of our ongoing study into designing effective heterogeneous catalysts for 5-HMF generation, we present the design and manufacture of a new catalyst,  $SiO_2$ -Imi- $SO_3H$ , *via* an accessible pathway, and the catalyst physicochemical characteristics were studied. This material was prepared by a method involving three steps as follows: grafting of chloropropyl groups to activated silica gel, the substitution of zwitterion, and the acidification of zwitterion to form silica-supported IL. The obtained catalyst showed high activity for 5-HMF production from fructose in DMSO at 140 °C. In addition, the optimization of process parameters such as the solvent nature, substrate scope, IL grafting degree, catalytic dosage, temperature, reaction time, and the recyclability of the catalyst were discussed. Next, the large-scale ability of the process and a mechanism were also proposed.

## Results and discussion

### Synthesis and characterization of the catalyst

The silica-supported IL  $SiO_2$ -Imi- $SO_3H$  was prepared through a three-step process illustrated in Scheme 2 (Experimental section). An acidic solution was used to activate the surface silanol groups on the silica gel surface.<sup>34</sup> Next, the reaction of activated silica gel with (3-chloropropyl)triethoxysilane was conducted under the catalysis of triethylamine to form 3-chloropropyl silica.<sup>35</sup> Next, the substitution of (3-chloropropyl)triethoxysilane and 4-(1H-imidazole-3-ium-3-yl)butane-1-sulfonate zwitterion was performed for 24 h to create a silica-supported zwitterion. Finally, the zwitterion was hydrochloric acid-treated to produce silica-supported IL. The catalyst was characterized by XRD, FT-IR, SEM, TGA, EDX, and elemental mapping. The  $SiO_2$ -Imi- $SO_3H$ -2 characterization results were represented in Fig. 1–4.

The successful surface modification of the silica gel surface was confirmed by FT-IR analysis (Fig. 1). The bands near 1090 and 802  $cm^{-1}$ , which were attributed to Si–O–Si bonds, were indicated in the  $SiO_2$ -Imi- $SO_3H$ -2 spectrum. The 2959 and 2933  $cm^{-1}$  doublets were ascribed to C–H stretching vibrations of propyl groups of silylating agent. In Fig. S3,<sup>†</sup> it can be

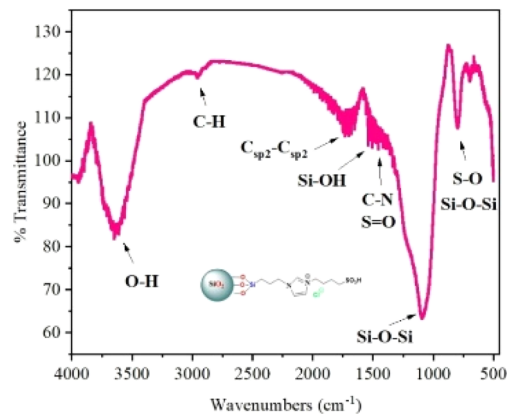


Fig. 1 FT-IR spectrum of  $SiO_2$ -Imi- $SO_3H$ -2.

observed that near 3000  $cm^{-1}$ , there was a signal of C–H bond in silica gel after the grafted silane chain (red line,  $SiO_2$ -Cl), which was not observed in the FT-IT spectrum of activated silica gel (black line, activated  $SiO_2$ ). This proved the successful grafting of the silane chain on activated silica gel. At 3400 and 954  $cm^{-1}$ , two signals were linked to O–H stretching and Si–OH. It should be noticed that the distinctive bands of  $-SO_3H$  groups overlapped with the Si–O–Si bands of silica gel.<sup>36</sup>

TGA was used to measure the weight loss of  $SiO_2$ -Imi- $SO_3H$ -2 as a function of temperature ranging from 25 to 800 °C in a nitrogen atmosphere (Fig. 2). There were two separate weight losses in the TGA diagram. First, the slight weight loss at temperatures lower than 250 °C was attributed to the removal of physically adsorbed solvent molecules. The major weight loss observed at 250–600 °C in the TGA diagram of  $SiO_2$ -Imi- $SO_3H$ -2 is mainly related to the decomposition of IL molecules grafted to the silica surface (18% of weight loss). When the temperature exceeded 600 °C, the sample weight remained unchanged, possibly due to the silica gel not being thermally decomposed. Therefore, the amount of silica gel in  $SiO_2$ -Imi- $SO_3H$ -2 was about 80%. Moreover,  $SiO_2$ -Imi- $SO_3H$ -2 could withstand the temperature of the reaction up to 250 °C.

The XRD pattern of  $SiO_2$ -Imi- $SO_3H$ -2 (Fig. 3a) showed a strong, broad diffraction peak at  $2\theta$  angle of 20–30° related to (222) planes of silica gel.<sup>37</sup> To probe the elemental composition

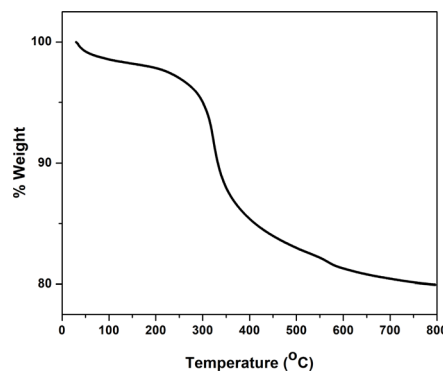


Fig. 2 TGA diagram of  $SiO_2$ -Imi- $SO_3H$ -2.

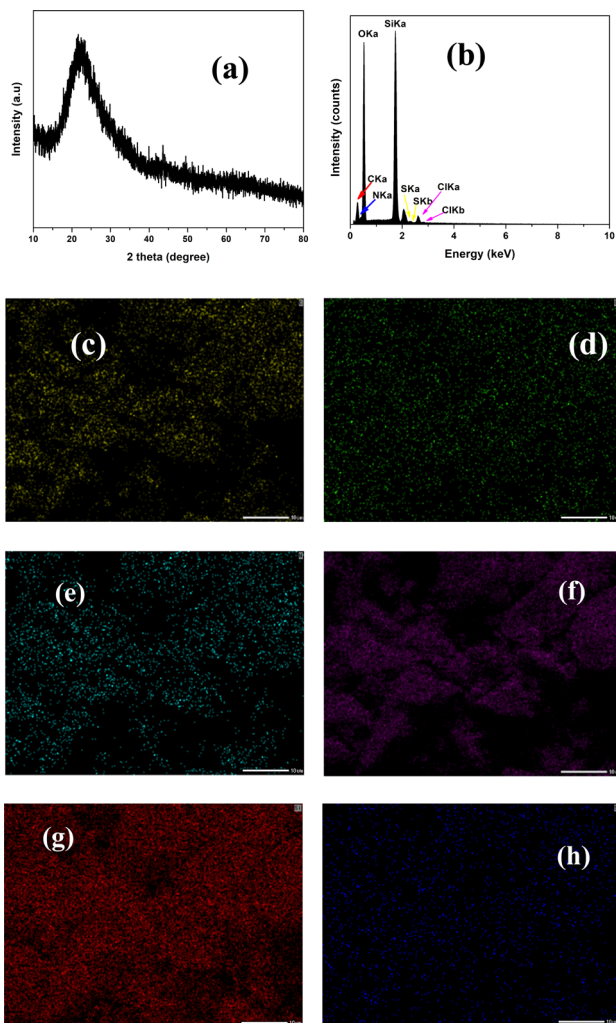


Fig. 3 Characterization of  $\text{SiO}_2\text{-Imi-SO}_3\text{H-2}$ : (a) XRD pattern; (b) EDX diagram; elemental distribution of (c) C element, (d) Cl element, (e) N element, (f) O element, (g) Si element, (h) S element.

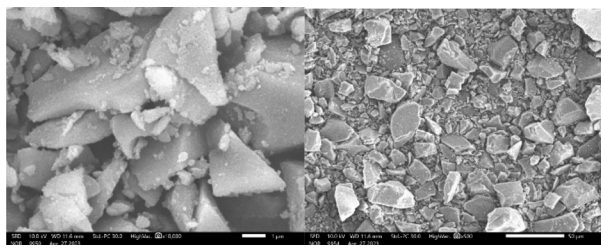


Fig. 4 SEM images at 1  $\mu\text{m}$  (left) and 50  $\mu\text{m}$  (right) magnifications of  $\text{SiO}_2\text{-Imi-SO}_3\text{H-2}$ .

of  $\text{SiO}_2\text{-Imi-SO}_3\text{H-2}$ , EDX spectroscopy was conducted, and the result is illustrated in Fig. 3b. The EDX spectrum of  $\text{SiO}_2\text{-Imi-SO}_3\text{H-2}$  revealed the peaks of Si, O, C, N, Cl, and S elements, illustrating the successful immobilization of sulfonated IL on silica gel. Furthermore, the EDX mapping study confirmed the uniform distribution of Si, O, C, and S components on the catalyst surface as presented in Fig. 3c–h. As can be observed in

Fig. 3h and g, silicone, and oxygen constitute the majority of silica gel-based materials.

To investigate the morphology of  $\text{SiO}_2\text{-Imi-SO}_3\text{H-2}$ , SEM analysis was conducted (Fig. 4). As can be seen,  $\text{SiO}_2\text{-Imi-SO}_3\text{H-2}$  was bulky, and the particles were micro-scale and had different sizes. According to FT-IR, TGA, EDX, SEM, elemental mapping, and XRD patterns, the grafting of IL on silica gel was proved, which was also our aim to synthesize  $\text{SiO}_2\text{-Imi-SO}_3\text{H-2}$ .

### Substrate scope

To initiate our investigation, we first examined the formation of 5-HMF from carbohydrates (fructose, glucose, sucrose, and cellulose). Conventional heating was implemented while using DMSO as the solvent. The results obtained are compared in Fig. 5. After 4 h of conventional heating, it was evident that the 5-HMF formation from fructose was significantly higher than that from glucose (70.0% and 1.2%, respectively). This difference could be attributed to the lack of active sites for glucose-to-fructose isomerization.<sup>36</sup>  $\text{SiO}_2\text{-Imi-SO}_3\text{H-2}$  also illustrated catalytic activity in the disaccharides, such as sucrose, dehydration, yielding 27.6% of 5-HMF, which was lower than the yield observed with the monosaccharide fructose (70.0%). This discrepancy is attributed to the multistep process involved in the formation of 5-HMF from disaccharides, encompassing hydrolysis, isomerization, and dehydration.<sup>38</sup> In contrast, the one-step synthesis of 5-HMF from sucrose offers a promising alternative for 5-HMF production, as it broadens the catalyst's substrate range and improves its long-term viability. However, the conversion of cellulose to 5-HMF (1.9%) is hindered due to the lack of Lewis acid sites or catalytic bases needed for the glucose-to-fructose isomerization process, resulting in a low yield of 5-HMF.

### Influence of solvents on the 5-HMF production

The choice of solvent is a critical factor in the synthesis of 5-HMF. In a comprehensive study investigating the impact of solvents on the fructose dehydration process to produce 5-HMF, a range of solvents, including polar and non-polar (water,

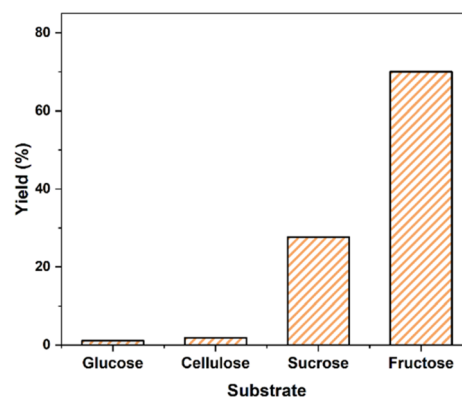


Fig. 5 The effect of different carbohydrates on 5-HMF production using  $\text{SiO}_2\text{-Imi-SO}_3\text{H-2}$ . Reaction conditions: substrate (1 mmol), catalyst (20 mg), DMSO (2 mL) at 120  $^{\circ}\text{C}$  for 4 h.



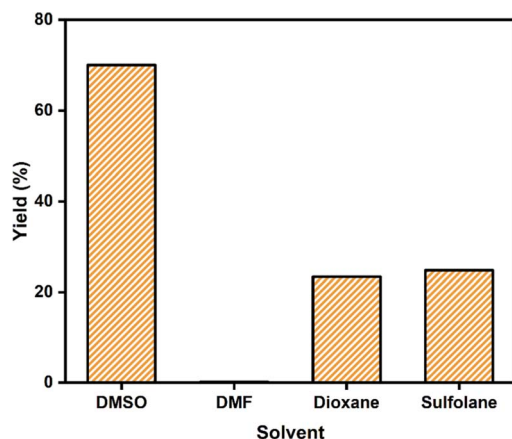


Fig. 6 The effect of different solvents on 5-HMF formation using  $\text{SiO}_2\text{-Imi-SO}_3\text{H-2}$ . Reaction conditions: fructose (1 mmol),  $\text{SiO}_2\text{-Imi-SO}_3\text{H-2}$  (20 mg), solvent (2 mL) at 120 °C for 4 h.

DMSO, *N,N*-dimethylformamide (DMF), 1,4-dioxane, and sulfolane) were utilized. The results are presented in Fig. 6.

It was observed that the lowest 5-HMF yield (0.15%) was obtained in DMF solvent, while the highest yield (70.0% within 4 h) was achieved in DMSO. This suggests that the 5-HMF produced in DMSO was stable, benefitting from the solvation impact, which minimized side processes by preserving the 5-HMF degradation.<sup>39</sup> In sulfolane and 1,4-dioxane solvents, the 5-HMF yields were approximately 24.8% and 23.8%, respectively. Finally, DMSO was selected as the reaction medium for further research.

#### Impact of IL grafting degree of the catalyst on 5-HMF yield

Three catalysts were synthesized with varying degrees of IL grafting onto activated silica gel, denoted as  $\text{SiO}_2\text{-Imi-SO}_3\text{H-1}$ ,  $\text{SiO}_2\text{-Imi-SO}_3\text{H-2}$ , and  $\text{SiO}_2\text{-Imi-SO}_3\text{H-3}$  in ascending order of IL grafting (in Experimental section). These catalysts were then utilized for the conversion of fructose to 5-HMF, and the results

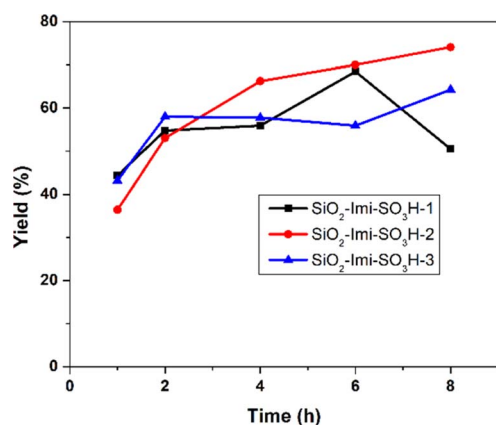


Fig. 7 Examination of IL grafting degree on 5-HMF yield. Reaction conditions: fructose (1 mmol); DMSO (2 mL);  $\text{SiO}_2\text{-Imi-SO}_3\text{H-1}$  (20 mg),  $\text{SiO}_2\text{-Imi-SO}_3\text{H-2}$  (20 mg), or  $\text{SiO}_2\text{-Imi-SO}_3\text{H-3}$  (20 mg); heating at 120 °C for 8 h.

are presented in Fig. 7. Analysis of the data reveals a notable influence of IL grafting amount on 5-HMF yield. Specifically, increasing the IL molar amount from 10 mmol to 20 mmol led to an increase in 5-HMF yield from 55.9% to 70.0% within 4 h (see Fig. 7). This enhancement in yield is attributed to a higher number of active acid sites, thereby augmenting the rate of fructose dehydration. However, a further increase in IL mole from 20 mmol to 30 mmol resulted in a decrease in 5-HMF yield under the same reaction conditions (70.0% and 57.6% after 4 h, respectively). This decline in 5-HMF production is ascribed to an excess of acidic sites, which promotes unwanted side reactions.<sup>40</sup> Notably, the  $\text{SiO}_2\text{-Imi-SO}_3\text{H-2}$  catalyst exhibited the highest 5-HMF yield of 81.7%, and thus was selected for subsequent experiments.

#### Impact of catalyst loading on the formation of 5-HMF

The dehydration of fructose was investigated at various concentrations of  $\text{SiO}_2\text{-Imi-SO}_3\text{H-2}$  to maximize 5-HMF formation.  $\text{SiO}_2\text{-Imi-SO}_3\text{H-2}$  amounts ranged from 5 to 50 mg, with a blank sample (without catalyst) included, whereas the rest of the conditions were kept unchanged as fructose (1 mmol) and DMSO (2 mL) at 120 °C. Fig. 8 illustrates the impact of  $\text{SiO}_2\text{-Imi-SO}_3\text{H-2}$  quantity on 5-HMF yield. The results revealed that the  $\text{SiO}_2\text{-Imi-SO}_3\text{H-2}$  dosage influenced the 5-HMF yield, generally increasing with higher catalyst amounts. Increasing the catalyst

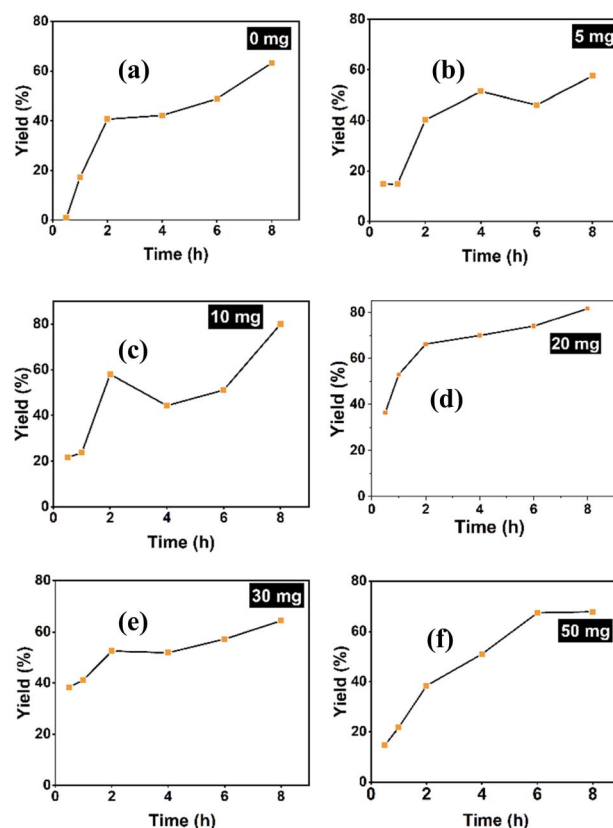


Fig. 8 Examination of catalyst loading on 5-HMF formation with (a) 0 mg (blank sample), (b) 5 mg, (c) 10 mg, (d) 20 mg, (e) 30 mg, (f) 50 mg, 120 °C, 8 h.

from 10 mg to 20 mg increased the 5-HMF yield from 51.1% to 74.1% within 6 h (Fig. 8c and d). This increase was attributed to the higher number of active acid sites, enhancing the rate of fructose dehydration. However, adjusting the amounts to 30 mg and 50 mg did not improve 5-HMF yields at the same reaction time (51.9% and 51.0% after 6 h, respectively) (Fig. 8e and f). This decline in 5-HMF production was attributed to excess acidic sites, leading to increased side products.<sup>40</sup> In the blank experiment, the 5-HMF yield was 42.2% after 4 h (Fig. 8a), lower than all  $\text{SiO}_2\text{-Imi-SO}_3\text{H-2}$  results when used as a catalyst. Notably, in the initial stage of the reaction (0.5–1 h), the blank sample's 5-HMF yields (0.8% and 17.2%, respectively) were much lower than those of samples using the catalysts (ranging from 12.9 to 53.0%), confirming the catalytic activity of  $\text{SiO}_2\text{-Imi-SO}_3\text{H-2}$ . The highest 5-HMF yield of 81.7% was achieved with a  $\text{SiO}_2\text{-Imi-SO}_3\text{H-2}$  catalyst amount of 20 mg after 8 h (Fig. 8d). Therefore, 20 mg was selected for further experiments.

### Effect of temperature on 5-HMF yield

The influences of temperature and time on the production of 5-HMF from fructose under the catalysis of  $\text{SiO}_2\text{-Imi-SO}_3\text{H-2}$  were evaluated. The reaction was carried out in DMSO containing fructose (1 mmol) and 20 mg of  $\text{SiO}_2\text{-Imi-SO}_3\text{H-2}$  at temperatures of 100 °C, 120 °C, 140 °C, and 160 °C. The obtained 5-HMF yields after 4 h were 40.0%, 70.0%, 74.5%, and 94.2%, respectively (Fig. 9).

The results demonstrate the significant influence of reaction temperature on 5-HMF yield. At 100 °C (Fig. 9a), 5-HMF yields were consistently lower than 60% at all reaction times, indicating that 100 °C was not suitable for the efficient fructose dehydration to 5-HMF. Increasing the temperature from 100 to 120 °C resulted in a notable rise in 5-HMF yield, from almost 0% to 36.4% within 0.5 h and from 40% to 71.0% within 4 h. This underscores the necessity of achieving a higher temperature than 100 °C for optimal 5-HMF yield.

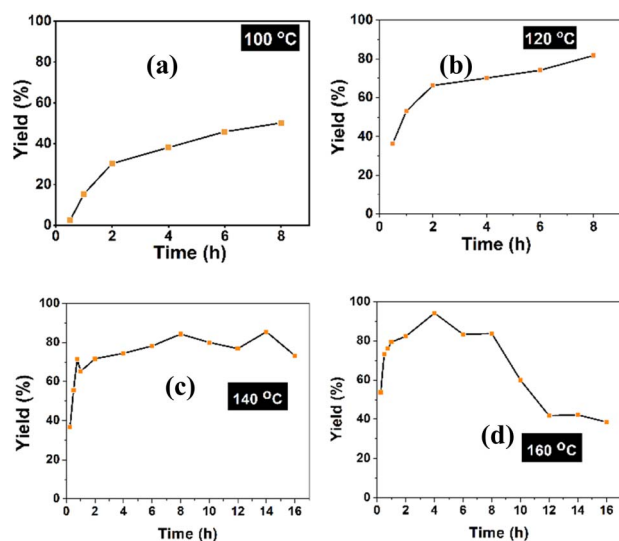


Fig. 9 Effect of temperature on 5-HMF yield. Reaction conditions: fructose (1 mmol), DMSO (2 mL),  $\text{SiO}_2\text{-Imi-SO}_3\text{H-2}$  (20 mg), heating at (a) 100 °C, (b) 120 °C for 8 h; (c) 140 °C, and (d) 160 °C for 16 h.

In Fig. 9a, at a temperature of 100 °C, 5-HMF yields were consistently below 60% for all reaction times, indicating that 100 °C was not optimal for the 5-HMF formation from fructose. It was illustrated in Fig. 9 that the increase in temperature from 100 to 120 °C led to an increase in 5-HMF yield from nearly 0% to 36.4% within 0.5 h and from 40% to 71.0% within 4 h. Therefore, achieving a higher 5-HMF yield required a temperature above 100 °C. At 140 °C and 160 °C, the initial stages of the reaction exhibited high 5-HMF yields (55.6% and 73.3%, respectively, after 0.5 h). Over time, the 5-HMF yields gradually increased to 84.3% after 8 h at 140 °C and 83.7% at 160 °C at the same reaction time (Fig. 9c and d). The highest 5-HMF yield, 94.2%, was obtained at 160 °C for a 4 hour reaction time (Fig. 9c). However, higher temperatures (140 °C and 160 °C) may also lead to the rapid byproducts formation, such as insoluble high-molecular-weight humins, which could be absorbed on the surface of  $\text{SiO}_2\text{-Imi-SO}_3\text{H-2}$ , thereby decreasing the catalytic activities of recovered catalysts. In Fig. 9d, after 8 h of reaction, 5-HMF yield decreased gradually, which may be attributed to the formation of humins. Therefore, 120 °C was chosen for the reusability examination of  $\text{SiO}_2\text{-Imi-SO}_3\text{H-2}$ .

### The examination of glucose transformation to 5-HMF with $\text{SiO}_2\text{-Imi-SO}_3\text{H-2}$

Next, we focused on the production of 5-HMF from a cheaper carbohydrate, glucose, to replace fructose as a starting material. Glucose was abundant and much cheaper than fructose. The process of producing 5-HMF from glucose begins with isomerization to fructose as glucose has a stable six-membered pyranose structure that resists dehydration,<sup>41</sup> but fructose is more reactive. Choudhary *et al.* discovered that Lewis acids may accelerate glucose dehydration to HMF by facilitating hydride transfer during glucose-to-fructose isomerization.<sup>42</sup> A catalyst having both types of catalytic sites is ideal for converting glucose to 5-HMF in one step, in which Brønsted acid catalyzes hydrolysis and dehydration, while Lewis acid promotes isomerization. According to Rasrendra *et al.*<sup>43</sup> and Yu *et al.*<sup>44</sup> the Lewis acid site indirectly enhances fructose dehydration *via* Brønsted acid, which is generated by metal hydrolysis in water. However, the indirect catalytic performance may vary depending on the reaction solvents used. In addition, the metal center with the highest electronegativity tended to increase fructose dehydration to 5-HMF, demonstrating its role in catalysis.<sup>44</sup>

Therefore, various Lewis salts such as  $\text{AlCl}_3 \cdot 6\text{H}_2\text{O}$ ,  $\text{CuCl}_2$ ,  $\text{FeCl}_3 \cdot 4\text{H}_2\text{O}$ ,  $\text{CrCl}_3 \cdot 6\text{H}_2\text{O}$ , or  $\text{ZnCl}_2$  were chosen as a co-catalyst to convert glucose to 5-HMF with  $\text{SiO}_2\text{-Imi-SO}_3\text{H-2}$  catalyst as Brønsted acid. The reaction conditions were glucose monohydrate (1 mmol),  $\text{SiO}_2\text{-Imi-SO}_3\text{H-2}$  (20 mg), DMSO (2 mL), and Lewis salts (20 mg) at a temperature of 120 °C within 4 h. As can be observed in Fig. 10, the 5-HMF yield from glucose with the catalysis of  $\text{AlCl}_3 \cdot 6\text{H}_2\text{O}$  was the highest (59.9%) compared to other salts. Compared to the result of glucose dehydration using only 20 mg of  $\text{SiO}_2\text{-Imi-SO}_3\text{H-2}$  as a catalyst (Fig. 5), 5-HMF yield with  $\text{AlCl}_3 \cdot 6\text{H}_2\text{O}$  afforded much higher 5-HMF yield than the sample without  $\text{AlCl}_3 \cdot 6\text{H}_2\text{O}$  (1.2%). Rasrendra *et al.*<sup>43</sup> also found that  $\text{CrCl}_3$ ,  $\text{CrCl}_2$ , and  $\text{AlCl}_3$  performed best in glucose



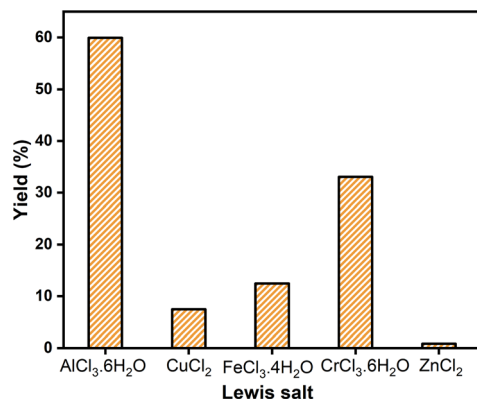


Fig. 10 Examination of the co-catalytic activities of various Lewis salts for the transformation of glucose to 5-HMF. Reaction conditions: glucose (1 mmol), DMSO (2 mL), SiO<sub>2</sub>-Imi-SO<sub>3</sub>H-2 (20 mg), and metal chloride (20 mg) at 120 °C for 4 h.

conversion in DMSO, yielding 54% and 52% 5-HMF, respectively. Certain metals were less effective. CuCl<sub>2</sub> created 0% HMF from glucose, while ZnCl<sub>2</sub> produced just 6% HMF in an organic solvent, which was relevant to the results of this study.<sup>43</sup> Further research is needed to identify the elements that influence performance variance.

These results also paved the way to broaden the application of SiO<sub>2</sub>-Imi-SO<sub>3</sub>H-2 as a catalyst for the conversion of much cheaper carbohydrates and glucose to 5-HMF with readily available Lewis salt AlCl<sub>3</sub>·6H<sub>2</sub>O. Moreover, the desirable 5-HMF yield from this process can also be employed for manufacturing on a large scale.

The product distribution was determined through the application of an HPLC method, specifically tailored for the quantification of 5-HMF along with two other common derivatives that may be formed in the reaction, namely 2,5-diformylfuran (DFF) and 2,5-furandicarboxylic (FDCA). The quantification of glucose conversion was conducted using the LC/MS/MS method. The comprehensive details of these analytical methods, including their conditions and formulas, are elaborated in the ESI Materials (S2).<sup>†</sup> Table 1 illustrates the product selectivities and glucose conversion achieved when employing SiO<sub>2</sub>-Imi-SO<sub>3</sub>H-2 and AlCl<sub>3</sub>·6H<sub>2</sub>O as catalysts for the conversion of glucose to 5-HMF. Notably, nearly complete

Table 1 The product selectivities and glucose conversion when SiO<sub>2</sub>-Imi-SO<sub>3</sub>H-2 and AlCl<sub>3</sub>·6H<sub>2</sub>O were utilized for the conversion of glucose to 5-HMF<sup>a</sup>

Time (h)	5-HMF selectivity (%)	DFF selectivity (%)	Glucose conversion (%)
0.5	41.7	0	100
1	42.5	0	100
2	52.8	0	100
3	52.7	4.0	100
4	59.5	5.0	100

<sup>a</sup> Reaction conditions: glucose (1 mmol), DMSO (2 mL), SiO<sub>2</sub>-Imi-SO<sub>3</sub>H-2 (20 mg), and AlCl<sub>3</sub>·6H<sub>2</sub>O (20 mg) at 120 °C for 4 h.

glucose conversion was observed after 0.5 h of reaction time. Initial detection of 5-HMF occurred shortly after this period, while DFF was first detected after 3 h. The selectivity towards DFF after 4 h remained low, below 5%, whereas no formation of FDCA was observed throughout the reaction.

### Evaluation of the SiO<sub>2</sub>-Imi-SO<sub>3</sub>H-2 recycling ability

The stability and reusability of SiO<sub>2</sub>-Imi-SO<sub>3</sub>H-2 catalyst impact the large-scale application of 5-HMF synthesis and the overall sustainability of the process. Fig. 11 displayed the FT-IR spectra of SiO<sub>2</sub>-Imi-SO<sub>3</sub>H-2 and the recycled SiO<sub>2</sub>-Imi-SO<sub>3</sub>H-2, showcasing the preservation of all functionalities of the original catalysts in the recovered ones.

The TGA curves for both the original and recovered SiO<sub>2</sub>-Imi-SO<sub>3</sub>H-2 are presented in Fig. 12. A comparison reveals distinct weight loss patterns between the two. The recovered SiO<sub>2</sub>-Imi-SO<sub>3</sub>H-2 exhibited an initial weight loss occurring below 100 °C, attributed to the removal of solvent molecules. Subsequently, a second weight loss was observed at around 150 °C in the recovered catalyst, possibly linked to the decomposition of humin molecules adsorbed onto the catalyst's surface. A third weight loss event was recorded at 300 °C, likely associated with the decomposition of the IL. Beyond 600 °C, the weight

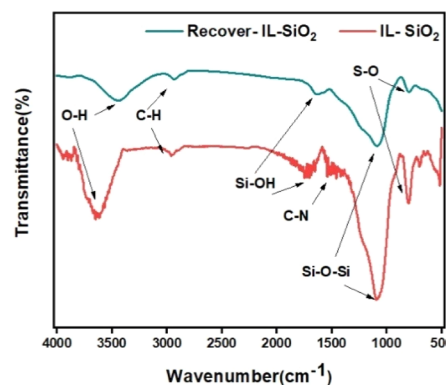


Fig. 11 FT-IR spectrum of recovered SiO<sub>2</sub>-Imi-SO<sub>3</sub>H-2.

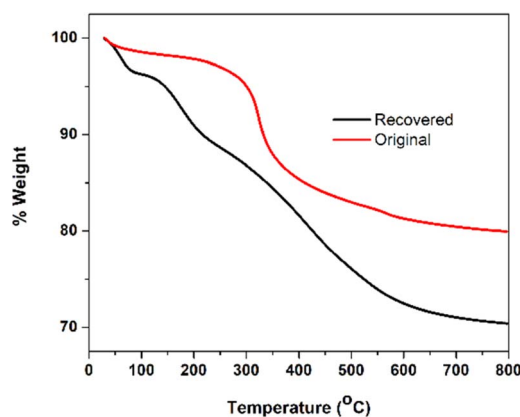


Fig. 12 TGA curves of original (red line) and recovered (black line) SiO<sub>2</sub>-Imi-SO<sub>3</sub>H-2.

remained constant, indicating that the amount of silica gel in the recovered  $\text{SiO}_2\text{-Imi-SO}_3\text{H-2}$  was approximately 70%, compared to the original  $\text{SiO}_2\text{-Imi-SO}_3\text{H-2}$ , which retained about 80% silica gel content. In summary, the attraction of humin and other solvents to the catalyst's surface resulted in a reduced silica gel content in the recovered catalyst compared to the original.

The XRD pattern of recovered  $\text{SiO}_2\text{-Imi-SO}_3\text{H-2}$  (Fig. 13a) also showed a strong, broad diffraction peak at  $2\theta$  angle of  $20\text{--}30^\circ$  related to (222) planes of silica gel, which proved that silica gel was still stable after the reaction.<sup>37</sup> EDX diagram of recovered  $\text{SiO}_2\text{-Imi-SO}_3\text{H-2}$  (Fig. 13b) revealed the peaks of Si, O, C, N, Cl, and S elements, illustrating all the elements were retained after the recovery. Additionally, the EDX mapping study confirmed the uniform distribution of Si, O, C, and S components on the catalyst surface as presented in Fig. 13c–h. It is noteworthy that in Fig. 13h and g, silicone, and oxygen constitute the majority of silica gel-based materials.

The mass percentages of all the elements in  $\text{SiO}_2\text{-Imi-SO}_3\text{H-2}$  and the recovered  $\text{SiO}_2\text{-Imi-SO}_3\text{H-2}$  are presented in Table S4.†

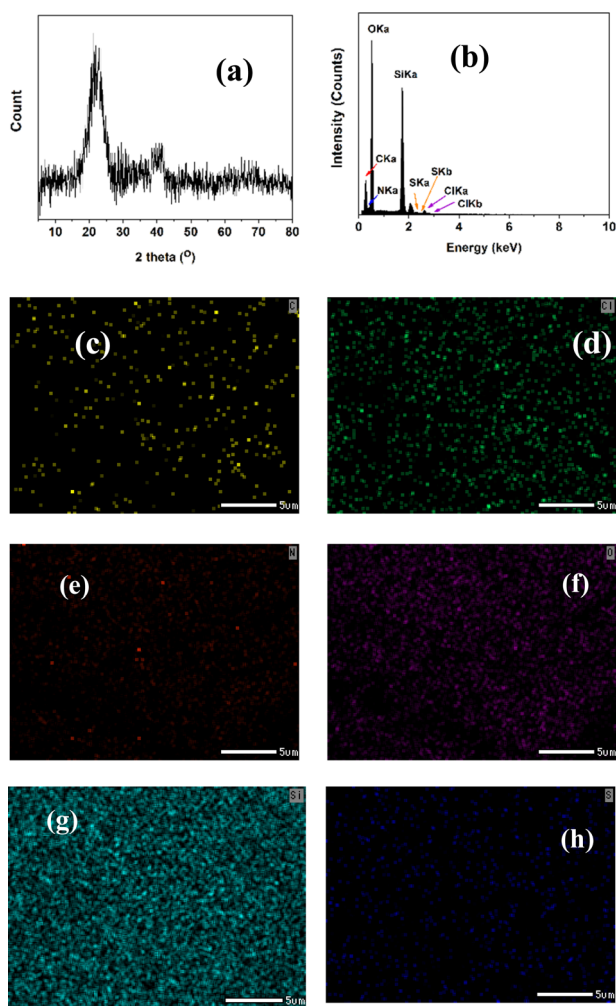


Fig. 13 Characterization of recovered  $\text{SiO}_2\text{-Imi-SO}_3\text{H-2}$ : (a) XRD pattern; (b) EDX diagram; elemental distribution of (c) C element, (d) Cl element, (e) N element, (f) O element, (g) Si element, (h) S element.

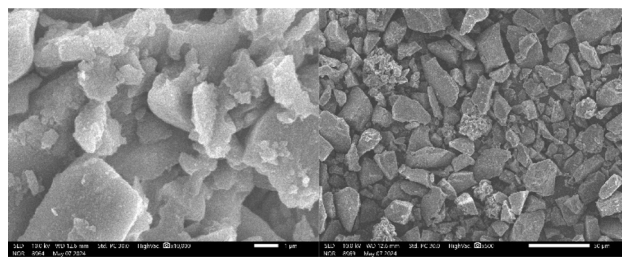


Fig. 14 SEM images at  $1\ \mu\text{m}$  (left) and  $50\ \mu\text{m}$  (right) magnifications of recovered  $\text{SiO}_2\text{-Imi-SO}_3\text{H-2}$ .

It is evident from the table that the mass percentages of N, Si, and Cl in the recovered catalyst decreased in comparison to those in the original catalyst. Conversely, the quantities of C and O elements in the recovered catalyst either remained approximately the same or were higher than those in the original catalyst. This observation suggests that during the recovery process, the IL may have been lost or that humin, a complex organic substance, was absorbed onto the surface of  $\text{SiO}_2\text{-Imi-SO}_3\text{H-2}$ . This absorption could have contributed to the increased mass percentage of the O element in the recovered catalyst.

SEM analysis was additionally performed to assess the morphology of the recovered  $\text{SiO}_2\text{-Imi-SO}_3\text{H-2}$ , as illustrated in Fig. 14. It is evident from the image that the recovered  $\text{SiO}_2\text{-Imi-SO}_3\text{H-2}$  retained its bulky structure, with particles exhibiting a micro-scale size and varying sizes among them. Based on these observations, it can be concluded that the morphology of the  $\text{SiO}_2\text{-Imi-SO}_3\text{H-2}$  catalyst remained unchanged throughout both the reaction and recovery stages.

The recyclability of  $\text{SiO}_2\text{-Imi-SO}_3\text{H-2}$  for dehydration of fructose to 5-HMF was assessed through a four-run recycling experiment. As depicted in Fig. 15, the 5-HMF yield only marginally fell from 85.9% to 70.2% after the third cycle. However, a significant decrease occurred after the fourth run, with the 5-HMF yield dropping to 44.4%. This decline can be attributed to the formation and buildup of humins on the

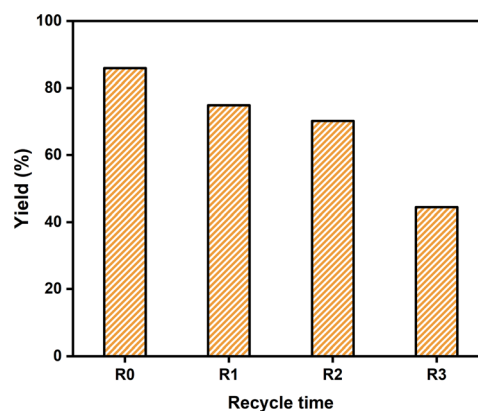


Fig. 15 Recyclability test of  $\text{SiO}_2\text{-Imi-SO}_3\text{H-2}$  for the 5-HMF formation from fructose. Reaction conditions: fructose (1 mmol),  $\text{SiO}_2\text{-Imi-SO}_3\text{H-2}$  (20 mg), DMSO (2 mL) at  $120^\circ\text{C}$  for 4 h.



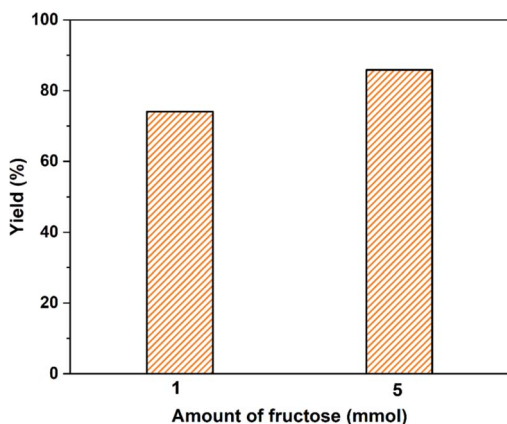


Fig. 16 A large-scale test of  $\text{SiO}_2\text{-Imi-SO}_3\text{H-2}$  for the 5-HMF production of fructose. Reaction conditions: fructose (900 mg), catalyst (100 mg), DMSO (15 mL) at 120 °C for 4 h.

catalyst surface, deactivating the active sites ( $-\text{SO}_3\text{H}$  groups), and decreasing 5-HMF yield.<sup>45,46</sup> Based on previous studies, 5-HMF has protonated by the Brønsted acid site<sup>47</sup> and formed humins from the self-condensation of 5-HMF, causing the reaction to change color. After the third run, the  $\text{SiO}_2\text{-Imi-SO}_3\text{H-2}$  surface is likely saturated with insoluble substances, contributing to minimal further changes in 5-HMF yield.

### The conversion of fructose into 5-HMF with $\text{SiO}_2\text{-Imi-SO}_3\text{H-2}$ on a larger scale

The 5-HMF production from fructose in DMSO on a larger scale (5 times) under the catalysis of  $\text{SiO}_2\text{-Imi-SO}_3\text{H-2}$  was examined, and the findings were depicted in Fig. 16. After the same reaction time, the large-scale sample gave a slightly higher 5-HMF yield than the standard one (Fig. 16). It can be said that a large amount of solvent did not strongly affect the dehydration of fructose, resulting in an approximate 5-HMF yield of two samples. These results indicate the potential application of  $\text{SiO}_2\text{-Imi-SO}_3\text{H-2}$  for industrial-scale processes.

### The $\text{SiO}_2\text{-Imi-SO}_3\text{H-2}$ catalyst in comparison to previous literature studies

Table 2 compares the results of fructose dehydration to 5-HMF under the catalysis of various silica-based catalysts in DMSO. The present method of using  $\text{SiO}_2\text{-Imi-SO}_3\text{H-2}$  catalyst for fructose dehydration to produce 5-HMF had a high yield of 5-HMF (94.1%) and better catalyst reusability with a smaller

amount ratio of fructose: catalyst. Finally, the present catalytic system proposed an efficient large-scale method for the production of 5-HMF, which made it applicable to other listed systems.

### The reaction mechanism for the transformation of fructose into 5-HMF using $\text{SiO}_2\text{-Imi-SO}_3\text{H}$

Various control experiments were conducted to examine the mechanism of the reaction. Activated silica gel (activated  $\text{SiO}_2$ ), activated silica gel grafted silane chain ( $\text{SiO}_2\text{-Cl}$ ),  $\text{SiO}_2\text{-Imi-SO}_3\text{H-2}$ , and blank reaction (without catalyst) were used as catalysts for the transformation of fructose to HMF in DMSO at 120 °C after 8 h. The results are depicted in Table 3.

As observed in Table 3, the inclusion of activated  $\text{SiO}_2$  and  $\text{SiO}_2\text{-Cl}$  did not significantly influence the dehydration process, as evidenced by comparing their HMF yields (entries 2 and 3) with that of the blank experiment (entry 1). In contrast, upon grafting IL onto silica gel, the HMF yield notably increased to 84.3% (entry 4), underscoring the crucial role played by  $-\text{SO}_3\text{H}$  groups on IL in catalyzing the conversion process. Moreover, the incorporation of materials grafted with IL facilitated an accelerated dehydration rate during the initial stages (refer to Fig. 8).

Scheme 1 depicts a possible chemical route for fructose dehydration mediated by  $\text{SiO}_2\text{-Imi-SO}_3\text{H}$ . The water removal was catalyzed by the sulfonic groups attached to the  $-\text{OH}$  in three successive steps *via* the E1 mechanism: two steps of 1,2-elimination and one step of 1,4-elimination reaction. Initially, fructose readily bonded to the outer surface of the  $\text{SiO}_2\text{-Imi-SO}_3\text{H}$  catalyst through hydrogen-bonding interactions involving the  $-\text{COOH}$  and  $-\text{OH}$  groups of  $\text{SiO}_2\text{-Imi-SO}_3\text{H}$  and the  $-\text{OH}$  groups of fructose. The predominantly Brønsted acid sites on the catalyst played a crucial role in the three-step dehydration of fructose.<sup>52</sup> This study found that the  $-\text{COOH}$  groups were primarily responsible for facilitating the 1,2- $\text{H}_2\text{O}$  elimination

Table 3 5-HMF yields of some controlled experiments<sup>a</sup>

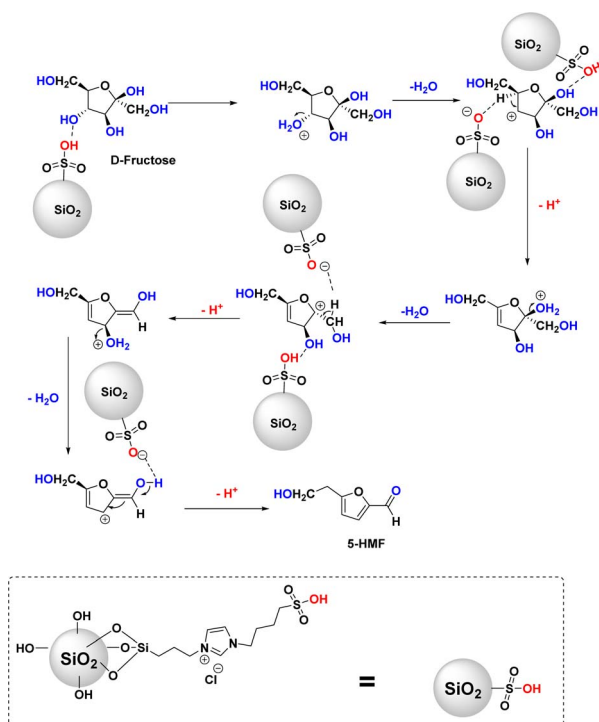
Entry	Catalyst	5-HMF yield (%)
1	None	63.3
2	Activated $\text{SiO}_2$	54.9
3	$\text{SiO}_2\text{-Cl}$	67.3
4	$\text{SiO}_2\text{-Imi-SO}_3\text{H-2}$	84.3

<sup>a</sup> Reaction conditions: fructose (1 mmol), catalyst (20 mg), DMSO (2 mL) at 120 °C for 8 h.

Table 2 The comparison of various silica-based catalysts for the synthesis of 5-HMF from fructose

Entry	Catalyst	Fructose amount (mg)	Temperature (°C)	Time (h)	Yield (%)	Ref.
1	SBA-15- $\text{SO}_3\text{H}$ (200)	100	120	1	96	48
2	COP- $\text{SO}_3\text{H/SB}$ (55)	100	120	1	80	49
3	$\text{Fe}_3\text{O}_4@\text{Si/PhSO}_3\text{H}$ (10)	20	110	3	82	50
4	Aquivion@silica (163)	300	120	1.5	85	51
7	$\text{SiO}_2\text{-Imi-SO}_3\text{H-2}$ (20 mg)	180	120	8	74.1	This work
8			160	4	94.2	





Scheme 1 Proposed pathway for the synthesis of 5-HMF using  $\text{SiO}_2\text{-Imi-SO}_3\text{H}$ .

through the E1 mechanism. Likewise, the presence of hydrogen bonds between the O–H bonds of fructose and  $\text{SiO}_2\text{-Imi-SO}_3\text{H}$  was believed to enhance the dehydration process, leading to the formation of an intermediate enol. Ultimately, a water molecule was eliminated through a 1,4-elimination reaction step, resulting in the production of 5-HMF.<sup>53</sup>

## Conclusions

Briefly, an IL was immobilized onto the activated silica gel by grafting chloropropyl groups on the activated silica gel, followed by the substitution of a zwitterion and acidification by chlorhydric acid. As-synthesized material ( $\text{SiO}_2\text{-Imi-SO}_3\text{H-2}$ ) was fully characterized by various analytical techniques such as EDX, XRD, FT-IR, SEM, TGA, and elemental mapping, which proved the successful immobilization of IL on silica gel.  $\text{SiO}_2\text{-Imi-SO}_3\text{H-2}$  was employed as a solid catalyst for the fructose transformation to 5-HMF. Various factors, including IL grafting degree, catalyst dosage, temperature, reaction duration, substrate range, and solvent, were evaluated, resulting in the refinement of reaction conditions through optimization. The maximum 5-HMF yield (94.1%) was achieved in DMSO solvent at 160 °C within 4 h. The catalyst's high recycling ability and durability were proven, and a mechanism for the process was also proposed.

## Experimental section

### Chemicals and materials

Except otherwise noted, all readily accessible substances were obtained from chemical sources and used exactly as given, with

no further treatment. Fructose (>99.5%), toluene (anhydrous, ≥99%), triethylamine (98%), and methanol (anhydrous, ≥99%) were purchased from Merck. Dimethyl sulfoxide (99.5%) was purchased from Fisher Scientific. Ethyl acetate (>99%), diethyl ether (>99%), and *n*-hexane (>99%) were purchased from Chemsol (Vietnam). Silica gel 230–400 mesh (37–63 μm) was purchased from Himedia (India). (3-chloropropyl)triethoxysilane (≥95%), 1,4-butane sultone (>99%), and deuteriochloroform (>99%) were purchased from Sigma-Aldrich.  $\text{AlCl}_3 \cdot 6\text{H}_2\text{O}$  (>98%), 1,4-dioxane (>99.5%), hydrochloric acid (36–38%), DMF (>99.5%), nitric acid (63%), D-glucose monohydrate (99%), and NaOH (≥98.0%) were supplied by Xilong. Imidazole (≥99.0%) was purchased from Kermel. Sulfolane (>99.0%) was supplied by Aladdin. Deionized (DI) water from the Millipore system (MilliQ®) was used in all the experiments.

### Catalyst preparation and characterization

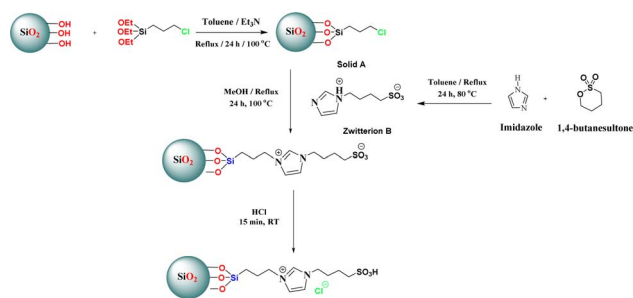
To activate silica gel, a mixture of silica gel and nitric acid (in a mole ratio of 1 : 2) was refluxed for 4 h. Subsequently, the silica gel was washed with distilled water until the pH reached approximately 7. Next, the silica gel was stirred in 4 M HCl solution at ambient temperature for 24 h. The activated silica gel was water-washed until the pH was approximately 7 and then dried at 100 °C in the oven for 24 h.<sup>54</sup> Next, a mixture of activated silica (6 g), (3-chloropropyl)triethoxysilane (2 g), triethylamine (1 mL), and a sufficient amount of toluene were placed inside a 100 mL round-bottom flask and heated at 110 °C for 24 h using a reflux system.<sup>54</sup> The resulting mixture was washed with diethyl ether (3 × 10 mL) (solid A).

Next, three molar amounts of 1,4-butane sultone (10, 20, or 30 mmol) were slowly added to a mixture of three molar amounts of imidazole (10, 20, or 30 mmol, respectively) and toluene in a 50 mL round-bottom flask equipped with a magnetic stirrer, and the reaction was refluxed for 24 h at 80 °C. The three mixtures were stirred until they became solid. The formed solids (zwitterion B1, B2, or B3, respectively) were then washed with diethyl ether (10 mL) three times and dried under vacuum at 50 °C.<sup>55</sup>

Next, solid A (5 g) and zwitterion B1, B2, or B3 were combined in a 50 mL flask with sufficient methanol and heated at 100 °C for 24 h. After completion of the reaction, the mixtures were evaporated to remove the solvent and eliminate impurities by washing with diethyl ether (3 × 10 mL). Subsequently, HCl (in sufficient quantity) was introduced to each mixture, and they were stirred at room temperature for another 15 min. After the reaction, each mixture was filtered, washed with DI water multiple times, and rinsed with ethanol. The resulting products were dried and stored at room temperature. Lastly, three ILs with Brønsted sites immobilized on silica gel were vacuum-dried for 6 h at 60 °C. The resulting catalysts were designated as  $\text{SiO}_2\text{-Imi-SO}_3\text{H-1}$ ,  $\text{SiO}_2\text{-Imi-SO}_3\text{H-2}$ , and  $\text{SiO}_2\text{-Imi-SO}_3\text{H-3}$  in accordance with the zwitterion moles of 10, 20, or 30 mmol (Scheme 2).

The thermal properties of  $\text{SiO}_2\text{-Imi-SO}_3\text{H-2}$  were examined by a TGA Instruments Q-500 with a heating rate of 10 K min<sup>−1</sup> from 25 °C to 800 °C in an  $\text{N}_2$  environment. FT-IR spectra of the



Scheme 2 Preparation of SiO<sub>2</sub>-Imi-SO<sub>3</sub>H.

catalysts in the 400–4000 cm<sup>−1</sup> wavenumber range were conducted on a JASCO FTIR-6600 using anhydrous KBr. XRD was performed using Cu K $\alpha$  radiation at 40 kV and 40 mA with 2 $\theta$  range from 5° to 80° and a scan rate of 4° min<sup>−1</sup>. Elemental compositions were determined using SEM-EDX mapping (JSM-IT200 SEM Series).

### Conditions for the experiments

The common procedure was carried out as follows: SiO<sub>2</sub>-Imi-SO<sub>3</sub>H-2 (20 mg), fructose (1 mmol), and DMSO (2 mL) were placed in a 15 mL round-bottom flask equipped with a screw cap and a magnetic stirrer. The process was subsequently permitted to operate at the specified temperature and time. At predetermined time intervals, 0.1 g of the reaction mixture was taken out and diluted with DI water for analysis using the UV-vis method on a JASCO V-670 UV-vis double-beam spectrophotometer (Japan). Absorbance values were recorded at 285.0 nm.<sup>56</sup> The procedure and calibration curve of 5-HMF at 285.0 nm are depicted in Section S1 of ESI.† The equation for determining the yield of 5-HMF is as follows:

$$\text{5-HMF yield (\%)} = \frac{\text{5-HMF moles}}{\text{initial fructose moles}} \times 100$$

The comparison between UV-vis and HPLC methods to quantify 5-HMF in this study is depicted in ESI S2†

In the reuse process, SiO<sub>2</sub>-Imi-SO<sub>3</sub>H-2 was separated by filtering, followed by the wash with DI water and ethyl acetate several times before being collected for the catalytic recycling experiment. The recycling experiment followed the same steps as previously stated.

### Author contributions

Vinh Thanh Chau Doan: investigation, data curation, methodology, writing – original draft, writing – review & editing. Thong Minh Dao: methodology, investigation, data curation. Thu Anh Huynh: methodology, investigation, data curation. The Thai Nguyen: investigation. Phuong Hoang Tran: methodology, writing – review & editing, supervision.

### Conflicts of interest

There are no conflicts to declare.

### Acknowledgements

This research is funded by the University of Science, VNU-HCM under grant number U2022-15.

### Notes and references

- 1 R. P. B. Ashok, P. Oinas and S. Forssell, *Renewable Energy*, 2022, **190**, 396–407.
- 2 J. N. Chheda, G. W. Huber and J. A. Dumesic, *Angew. Chem., Int. Ed.*, 2007, **46**, 7164–7183.
- 3 G. W. Huber, J. N. Chheda, C. J. Barrett and J. A. Dumesic, *Science*, 2005, **308**, 1446–1450.
- 4 Y. Y. Gorbanev, S. Kegnæs and A. Riisager, *Top. Catal.*, 2011, **54**, 1318–1324.
- 5 Y. Meng, S. Yang and H. Li, *ChemSusChem*, 2022, **15**, e202102581.
- 6 S. Mu, K. Liu, H. Li, Z. Zhao, X. Lyu, Y. Jiao, X. Li, X. Gao and X. Fan, *Fuel Process. Technol.*, 2022, **233**, 107292.
- 7 S. Mondal, J. Mondal and A. Bhaumik, *ChemCatChem*, 2015, **7**, 3570–3578.
- 8 H. Ma, Z. Li, L. Chen and J. Teng, *RSC Adv.*, 2021, **11**, 1404–1410.
- 9 J. N. Chheda, Y. Román-Leshkov and J. A. Dumesic, *Green Chem.*, 2007, **9**, 342–350.
- 10 M. Sajid, Y. Bai, D. Liu and X. Zhao, *Arabian J. Chem.*, 2020, **13**, 7430–7444.
- 11 C. Moreau, R. Durand, S. Razigade, J. Duhamet, P. Faugeras, P. Rivalier, P. Ros and G. Avignon, *Appl. Catal., A*, 1996, **145**, 211–224.
- 12 H. Zhao, J. E. Holladay, H. Brown and Z. C. Zhang, *Science*, 2007, **316**, 1597–1600.
- 13 T. Armaroli, G. Busca, C. Carlini, M. Giuttari, A. M. R. Galletti and G. Sbrana, *J. Mol. Catal. A: Chem.*, 2000, **151**, 233–243.
- 14 C. Carlini, M. Giuttari, A. M. R. Galletti, G. Sbrana, T. Armaroli and G. Busca, *Appl. Catal., A*, 1999, **183**, 295–302.
- 15 F. Benvenuti, C. Carlini, P. Patrono, A. M. R. Galletti, G. Sbrana, M. A. Massucci and P. Galli, *Appl. Catal., A*, 2000, **193**, 147–153.
- 16 Y. Román-Leshkov, J. N. Chheda and J. A. Dumesic, *Science*, 2006, **312**, 1933–1937.
- 17 C. Lansalot-Matras and C. Moreau, *Catal. Commun.*, 2003, **4**, 517–520.
- 18 J. N. Chheda, Y. Román-Leshkov and J. A. Dumesic, *Green Chem.*, 2007, **9**, 342–350.
- 19 Y. Nakamura and S. Morikawa, *Bull. Chem. Soc. Jpn.*, 1980, **53**, 3705–3706.
- 20 L. Lin, X. Han, B. Han and S. Yang, *Chem. Soc. Rev.*, 2021, **50**, 11270–11292.
- 21 X. Lyu, H. Li, H. Xiang, Y. Mu, N. Ji, X. Lu, X. Fan and X. Gao, *Chem. Eng. J.*, 2022, **428**, 131143.
- 22 S. K. Kundu and A. Bhaumik, *ACS Sustain. Chem. Eng.*, 2015, **3**, 1715–1723.
- 23 P. Ghamari Kargar, G. Bagherzade and M. Ghasemi, *Medbiotech J.*, 2021, **5**, 9–14.
- 24 P. Ghamari Kargar, M. Ghasemi and G. Bagherzade, *Sci. Iran.*, 2022, **29**, 1338–1350.



- 25 V. T. C. Doan, T. H. Nguyen, H. B. Phan and P. H. Tran, *Mol. Catal.*, 2023, **549**, 113518.
- 26 Q. Zhao, L. Wang, S. Zhao, X. Wang and S. Wang, *Fuel*, 2011, **90**, 2289–2293.
- 27 F. Shi, Q. Zhang, D. Li and Y. Deng, *Chem.–Eur. J.*, 2005, **11**, 5279–5288.
- 28 C. Romero and S. Baldelli, *J. Phys. Chem. B*, 2006, **110**, 6213–6223.
- 29 T. Huang, H.-x. Zhang, X.-h. Zhang, D.-y. Peng, X.-l. Nie, J. Chen and W.-m. Xiong, *J. Mol. Liq.*, 2022, **345**, 118233.
- 30 S. Eminov, J. D. E. T. Wilton-Ely and J. P. Hallett, *ACS Sustain. Chem. Eng.*, 2014, **2**, 978–981.
- 31 S. Sahoo, P. Kumar, F. Lefebvre and S. B. Halligudi, *Appl. Catal., A*, 2009, **354**, 17–25.
- 32 L. Zhu, Y. Liu and J. Chen, *Ind. Eng. Chem. Res.*, 2009, **48**, 3261–3267.
- 33 W. Chen, Y. Zhang, L. Zhu, J. Lan, R. Xie and J. You, *J. Am. Chem. Soc.*, 2007, **129**, 13879–13886.
- 34 M. Gharehbaghi and F. Shemirani, *Anal. Methods*, 2012, **4**, 2879–2886.
- 35 A. S. Amarasekara and O. S. Owereh, *Catal. Commun.*, 2010, **11**, 1072–1075.
- 36 M. Niakan, M. Masteri-Farahani and F. Seidi, *Fuel*, 2023, **337**, 127242.
- 37 M. F. Elkady, H. S. Hassan and A. M. Hashim, *Jokull J.*, 2015, **65**, 390–417.
- 38 M. Niakan, M. Masteri-Farahani, S. Karimi and H. Shekaari, *Sustainable Energy Fuels*, 2022, **6**, 2514–2522.
- 39 X. Tong and Y. Li, *ChemSusChem*, 2010, **3**, 350–355.
- 40 X. Zhang, D. Zhang, Z. Sun, L. Xue, X. Wang and Z. Jiang, *Appl. Catal., B*, 2016, **196**, 50–56.
- 41 L. Hu, G. Zhao, X. Tang, Z. Wu, J. Xu, L. Lin and S. Liu, *Bioresour. Technol.*, 2013, **148**, 501–507.
- 42 V. Choudhary, A. B. Pinar, R. F. Lobo, D. G. Vlachos and S. I. Sandler, *ChemSusChem*, 2013, **6**, 2369–2376.
- 43 C. B. Rasrendra, J. N. M. Soetedjo, I. Makertihartha, S. Adisasmito and H. J. Heeres, *Top. Catal.*, 2012, **55**, 543–549.
- 44 I. K. M. Yu, D. C. W. Tsang, A. C. K. Yip, S. S. Chen, Y. S. Ok and C. S. Poon, *Bioresour. Technol.*, 2016, **219**, 338–347.
- 45 F. Guo, Z. Fang and T.-J. Zhou, *Bioresour. Technol.*, 2012, **112**, 313–318.
- 46 X. Qi, N. Liu and Y. Lian, *RSC Adv.*, 2015, **5**, 17526–17531.
- 47 Y. Qu, Q. Wei, H. Li, P. Oleskowicz-Popiel, C. Huang and J. Xu, *Bioresour. Technol.*, 2014, **162**, 358–364.
- 48 L. Wang, L. Zhang, H. Li, Y. Ma and R. Zhang, *Composites, Part B*, 2019, **156**, 88–94.
- 49 Z. Babaei, A. N. Chermahini, M. Dinari, M. Saraji and A. Shahvar, *Sustainable Energy Fuels*, 2019, **3**, 1024–1032.
- 50 X. Zhang, M. Wang, Y. Wang, C. Zhang, Z. Zhang, F. Wang and J. Xu, *Chin. J. Catal.*, 2014, **35**, 703–708.
- 51 Y. Dou, S. Zhou, C. Oldani, W. Fang and Q. Cao, *Fuel*, 2018, **214**, 45–54.
- 52 I. Elsayed, M. Mashaly, F. Eltaweel and M. A. Jackson, *Fuel*, 2018, **221**, 407–416.
- 53 M. L. Testa, G. Miroddi, M. Russo, V. La Parola and G. Marci, *Materials*, 2020, **13**, 1178.
- 54 F. Adam, H. Osman and K. M. Hello, *J. Colloid Interface Sci.*, 2009, **331**, 143–147.
- 55 N. G. Khaligh, O. C. Ling, M. R. Johan and J. J. Ching, *J. Mol. Struct.*, 2019, **1180**, 280–284.
- 56 C. Chi, Z. Zhang, H.-m. Chang and H. Jameel, *J. Wood Chem. Technol.*, 2009, **29**, 265–276.

